

CHEMISTRY

A European Journal

A Journal of



Accepted Article

Title: The Construction of Homochiral Lanthanide Quadruple-Stranded Helicates with Multi-Responsive Sensing Properties toward Fluoride Anions

Authors: Wanmin Chen, Xiaoliang Tang, Wei Dou, Bei Wang, Lirong Guo, Zhenghua Ju, and Weisheng Liu

This manuscript has been accepted after peer review and appears as an Accepted Article online prior to editing, proofing, and formal publication of the final Version of Record (VoR). This work is currently citable by using the Digital Object Identifier (DOI) given below. The VoR will be published online in Early View as soon as possible and may be different to this Accepted Article as a result of editing. Readers should obtain the VoR from the journal website shown below when it is published to ensure accuracy of information. The authors are responsible for the content of this Accepted Article.

To be cited as: *Chem. Eur. J.* 10.1002/chem.201700827

Link to VoR: <http://dx.doi.org/10.1002/chem.201700827>

Supported by
ACES

WILEY-VCH

The Construction of Homochiral Lanthanide Quadruple-Stranded Helicates with Multi-Responsive Sensing Properties toward Fluoride Anions

Wanmin Chen, Xiaoliang Tang,* Wei Dou, Bei Wang, Lirong Guo, Zhenghua Ju, and Weisheng Liu*^[a]

Abstract: A series of unique homochiral lanthanide tetranuclear quadruple-stranded helicates have been self-assembled controllably by taking the intrinsic advantages of chiral bridging ligands, (*S*)-H₂L and (*R*)-H₂L, and lanthanide ions with high coordination numbers. The self-assembly process of these chiral helicates not only ensures the structural stability and quadruple-stranded feature of lanthanide cluster in solid and solution, but also achieves the effective transfer and amplification of chirality code from ligand to higher supramolecular level. Moreover, through using optical rotation, circular dichroism spectra analysis and luminescence measurement, we demonstrate that these chiral lanthanide helicates could serve as sensitive and multi-responsive sensors to recognize and detect F⁻ anions based on the change of chiral signal and NIR luminescence simultaneously, which represents a meaningful exploration for developing functional lanthanide-based polynuclear clusters.

Introduction

Chirality is one of the intrinsic features of nature and plays such a vital role in natural and life sciences that it is called signature of life.^[1] Many efforts have been devoted to the structural design and utilization of enantiopure compounds or supramolecular assemblies^[2] due to the strong demand for chiral properties in the fields of asymmetric catalysis, enantioselective separation, nonlinear optical materials, bioscience and pharmaceuticals.^[3]

Among various strategies to synthesize chiral substances, transition metal center-directed self-assembly incorporated with chiral functional groups in ligand not only provides directly excellent opportunities to widen the research scope of chiral materials, but also establishes a platform for chirality induction, inversion and transfer.^[4] There is a great deal of progress in the construction of chiral transition metal complexes, such as helicates,^[5] cage complexes,^[6] coordination polymers,^[7] and metal-organic frameworks (MOFs).^[8] However, the research of chiral lanthanide complexes, especially chiral polynuclear clusters, is less well understood,^[9] although lanthanide ions possess special electronic configuration and their complexes are ideal candidates for fascinating structures and potential

applications in superconductive, magnetic, optical, electronic, and catalytic processes.^[10] The main reasons may be due to uncontrollability of polynuclear arrangement and inherent nature of lanthanide ions, including their high coordination numbers, kinetic lability, weak stereochemical preference and more variable nature of the coordination sphere, which might exhibit uncertain stereochemistry so that the molecular structures and frameworks of lanthanide complexes could not be well regulated or predicted.^[9,10] Lehn, Bünzli, Piguet, Gunnlaugsson and a few pioneers have investigated a series of lanthanide helicates constructed by multidentate ligands in detail and focused on the preparation of helicates,^[10,11] but the controllable self-assembly and application of chiral lanthanide-based polynuclear helicates accompanied with chiral signal change also remain a great challenge and need to be explored further.

On the other hand, the signal transduction for selectively recognizing or detecting anions is a significant topic in analysis technology as well as environmental science.^[12] As one of the essential microelements in the human body, a certain amount of F⁻ as additive in toothpastes and water can prevent dental caries effectively, but excessive ingestion of F⁻ may cause fluorosis, leading to a series of skeletal diseases, mottled teeth, kidney disorders and urolithiasis.^[13] Therefore, the monitoring of F⁻ with high electronegativity has received considerable attention.^[14] At present, most of F⁻-selective signal recognition studies are based on ion chromatography and fluorescent chemosensor, but other detection methods are rarely employed and exploited.^[15] Thus, the utilization of chirality signal to trace F⁻ may be a promising and new strategy, which provides a beneficial supplement for F⁻-selective recognition in analytical method.

We have been interested in the construction of novel chiral lanthanide helicates through using enantiomorphous ligands to develop new recognition function.^[9b,9e] To controllably prepare lanthanide-based polynuclear helicates and extend application of chiral complex in information transfer, a pair of homochiral bridging ligands, (*S*)-H₂L and (*R*)-H₂L ((1*S*, 2*S*)- and (1*R*, 2*R*)-*N*¹,*N*²-bis(3-ethoxy-2-hydroxybenzylidene)cyclohexane-1,2-dicarbohydrazide), were designed by the introduction of enantiomerically pure and disubstituted cyclohexyl group. Two enantiomorphous ligands with rigid and folded framework possess acylhydrazone groups linked together with phenol moiety at the two termini, which not only provides tridentate coordination site to capture lanthanide ion, but also can transfer directly energy to sensitize the luminescence of metal ion as antenna group. Moreover, the existence of two hydroxyl oxygen atoms and two ether oxygen atoms could bridge other lanthanide ions to form polynuclear arrangement.

Herein, we report two pair of unique and enantiomerically pure chiral lanthanide-based tetranuclear quadruple-stranded helicates, which are self-assembled by different lanthanide ions and homochiral ligands with the aid of NO₃⁻ anion template under mild conditions. And more importantly, the homochiral

[a] W. Chen, Dr. X. Tang, Dr. W. Dou, B. Wang, L. Guo, Z. Ju, Prof. Dr. W. Liu

Key Laboratory of Nonferrous Metal Chemistry and Resources Utilization of Gansu Province and State Key Laboratory of Applied Organic Chemistry, Key Laboratory of Special Function Materials and Structure Design, Ministry of Education, College of Chemistry and Chemical Engineering, Lanzhou University, Lanzhou, 730000, China
Fax: (+86) -931-8912582
E-mail: tangxiaol@lzu.edu.cn, liuws@lzu.edu.cn

Supporting information for this article is given via a link at the end of the document. ((Please delete this text if not appropriate))

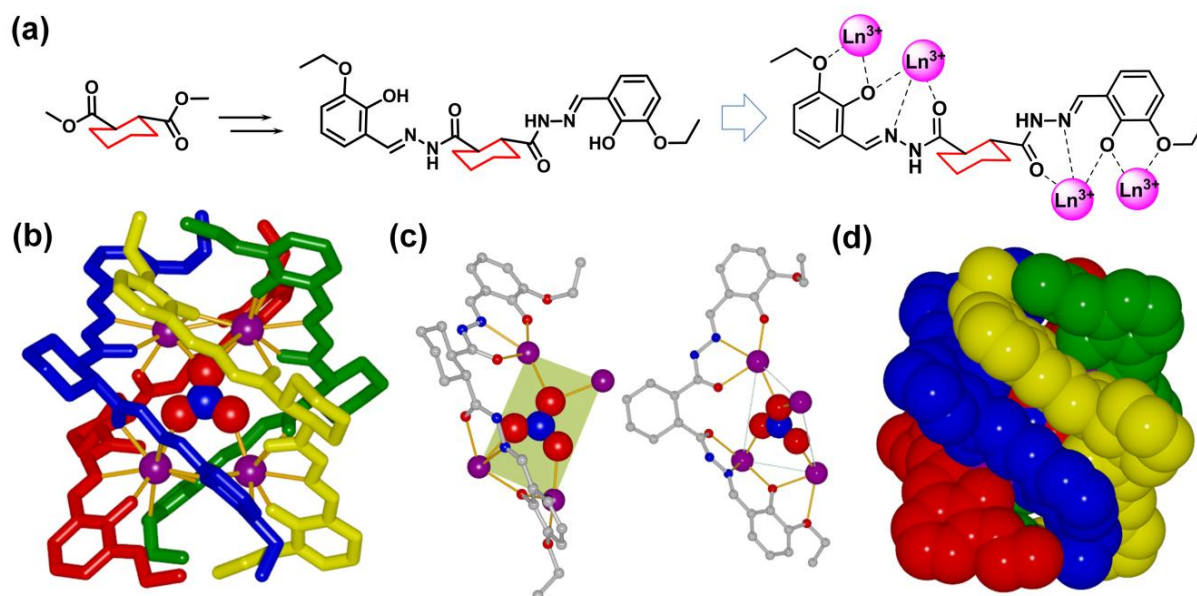


Figure 1. a) Synthesis of a homochiral bridging ligand by the introduction of disubstituted and enantiomerically pure cyclohexyl group, and structural formula of the chiral ligand with potential multi coordination sites capturing lanthanide ions. b) Capped sticks representation of $[\text{La}_4\{(\text{R})\text{-L}\}_4(\text{NO}_3)]^{3+}$ (**1a**) containing four La^{3+} ions and four $(\text{R})\text{-L}^{2-}$ ligands. The triangular NO_3^- ion is encapsulated by ligands and shown in a space-filling representation. Each of ligand is represented in a different color, and element La is violet. c) The coordination pattern of each ligand $(\text{R})\text{-L}^{2-}$ in helicate from different perspectives. All four La^{3+} ions are bridged by NO_3^- ion to form a twisted rectangle. d) Space-filling representation of the homochiral lanthanide tetranuclear quadruple-stranded *M* helical structure.

lanthanide helicate further displayed high selectivity toward F^- in chiral signal as well as turn-on luminescent response in near-infrared region, which represents the successful exploitation of the chiral lanthanide supramolecular structure and function.

Results and Discussion

Synthesis of chiral lanthanide helicates

The chiral bridging ligands, $(\text{R})\text{-H}_2\text{L}$ and $(\text{S})\text{-H}_2\text{L}$, were first prepared by the reaction of chiral $(1\text{R}, 2\text{R})$ and $(1\text{S}, 2\text{S})$ -cyclohexane-1,2-dicarbohydrazone with 3-ethoxy-2-hydroxybenzaldehyde, respectively (Figure 1a and Scheme S1). Then, single chiral quadruple-stranded helicates were synthesized by the addition of a solution of $\text{Ln}(\text{NO}_3)_3 \cdot 6\text{H}_2\text{O}$ ($\text{Ln} = \text{La}, \text{Nd}$) in methanol to a pale yellow and transparent solution of $(\text{R})\text{-H}_2\text{L}$ or $(\text{S})\text{-H}_2\text{L}$ and $\text{LiOH} \cdot \text{H}_2\text{O}$ (1:2 molar ratio) in a mixed solution of methanol and acetonitrile. Yellow diamond crystals of $[\text{Ln}_4\{(\text{R})\text{-L}\}_4(\text{NO}_3)] \cdot 3\text{NO}_3 \cdot x\text{CH}_3\text{OH} \cdot y\text{H}_2\text{O} \cdot z\text{CH}_3\text{CN}$ ($\text{Ln} = \text{La}$ (**1a**), Nd (**2a**)) or $[\text{Ln}_4\{(\text{S})\text{-L}\}_4(\text{NO}_3)] \cdot 3\text{NO}_3 \cdot x\text{CH}_3\text{OH} \cdot y\text{H}_2\text{O} \cdot z\text{CH}_3\text{CN}$ ($\text{Ln} = \text{La}$ (**1b**), Nd (**2b**)) suitable for X-ray diffraction were obtained in good yield by slow evaporation of the solution in air at room temperature within a week.

Structural features of chiral helicates

X-ray crystallographic analysis revealed that four quadruple-stranded helicates **1a**, **1b**, **2a** and **2b** crystallized in chiral space groups (Table S1). In all compounds, the helical cluster cations, $[\text{Ln}_4\text{L}_4(\text{NO}_3)]^{3+}$ ($\text{L} =$ the deprotonated ligand $(\text{R})\text{-L}^{2-}$ or $(\text{S})\text{-L}^{2-}$), are similar and each of them is composed of four deprotonated chiral ligands, four lanthanide ions, and an encapsulated nitrate in the center. Therefore, the crystal structure of **1a** is depicted here in detail for the sake of brevity.

In the cluster $[\text{La}_4\{(\text{R})\text{-L}\}_4(\text{NO}_3)]^{3+}$, disubstituted cyclohexyl group with boat form in the middle of ligand restrains the variety of ligand chain, and whole ligand presents rigid and V-shaped framework. The acylhydrazone group accompanied with phenol moiety provides tridentate coordination fashion, and two La^{3+} ions are captured effectively into tridentate coordination sites, respectively, on both ends of rigid ligand (Figure 1b). Each of La^{3+} ions is chelated by two acylhydrazone moieties from different ligands, and is further chelated by the deprotonated phenolic oxygen atom and ether oxygen atom from the third ligand in a bidentate mode. In addition, the nitrate group in the center of cluster offers oxygen atoms participates in the coordination of La^{3+} ions, and finally the coordination polyhedra around each of La^{3+} ions can be best described as slightly distorted tricapped trigonal prisms (Figure S1). Four La^{3+} ions form a slightly twisted rectangle and they could be divided into two groups, in each of which two closer La^{3+} ions are bridged by two deprotonated phenolic oxygen atoms to form double metal cluster unit, and the distances of $\text{La} \cdots \text{La}$ are 3.99 Å and 4.08 Å, respectively (Figure 1c). Two pairs of double metal clusters are linked and wrapped by four ligands, and the distances of $\text{La} \cdots \text{La}$ as longer side of twisted rectangle are 5.99 Å and 6.12

Å, respectively. Thus, all chiral bridging ligands twine orderly around four lanthanide ions along the fixed spiral direction, resulting in the formation of homochiral tetranuclear quadruple-stranded *M* helicate structure (Figure 1d). That is, the chirality code of ligand is effectively transferred and amplified towards the higher supramolecular level with the participation of lanthanide ions.

Another notable structural feature of these helicates is that all four La^{3+} ions are coordinated and linked closely by the central NO_3^- anion, which adopts a $\mu_4\text{-}\eta^1\eta^1\eta^2$ bridging mode as second ligand. As shown in Figure 1c, one of oxygen atoms in nitrate bridges two lanthanide ions and the other two oxygen atoms coordinate with the rest two lanthanide ions, respectively. The $\text{La} \cdots \text{O}$ distances are within the normal range of 2.59 Å to 2.66 Å. The bridging NO_3^- anion occupies the nucleation site of cluster $[\text{La}_4\{(R)\text{-L}\}_4(\text{NO}_3)]^{3+}$, and serves as an important template part in self-assembly of the chiral quadruple-stranded helicate. In other words, the homochiral cluster structure is further stabilized by the introduction of the NO_3^- anion.

Characterization of chiral lanthanide helicates

The self-assembly of chiral helicates and the template effect of the NO_3^- anion in the cluster core were further investigated by using IR, NMR and mass spectrographic analysis. FT-IR spectra of all helicates in solid state showed clearly that the characteristic strong bands for stretch vibrations $\nu(\text{C}=\text{O})$ at 1660 cm^{-1} and $\nu(\text{Ar}-\text{OH})$ at 1250 cm^{-1} of free ligands shift towards lower wave numbers by $\sim 30\text{ cm}^{-1}$ and $\sim 32\text{ cm}^{-1}$, respectively, indicating that amide groups and phenol groups in ligand take part in coordination to lanthanide ions and result in the formation of new structure. In addition, strong nitrate-based vibrations at 1384 cm^{-1} , which are not observed for ligands, are presented in the spectra of helicates, suggesting that NO_3^- anions are fixed firmly in complexes (Figure S2).

In order to discuss the role NO_3^- plays, LaCl_3 was employed to replace $\text{La}(\text{NO}_3)_3$ and react with deprotonated (*R*)- H_2L at the early stage during preparation process of complex, and then, NaNO_3 in methanol was added. The obtained crystals were consistent with chiral tetranuclear quadruple-stranded cluster **1a**, which was confirmed by X-ray crystallographic analysis. Meanwhile, ^{15}N isotopic labeled NaNO_3 was used and solid-state ^{15}N NMR spectrum showed clearly that a weak peak with low intensity appeared at $\delta = 384.12$ ppm, which can be ascribed to the encapsulated NO_3^- in the center of helicate (Figure S3). Thus, strong binding ability of NO_3^- in tetranuclear quadruple-stranded cluster structure was revealed and the important templating function of NO_3^- anion was well presented.

To confirm the stability of these chiral tetranuclear quadruple-stranded helicates in the solution, high-resolution electrospray ionization mass spectra (HRESI-MS) of **1a** was performed. As shown in Figure 2, the presence of the intense peaks at $m/z = 864.8266$ with isotopic distribution patterns separated by $(0.33 \pm 0.005)\text{ Da}$ easily belongs to positively charged $[\text{La}_4\{(R)\text{-L}\}_4(\text{NO}_3)]^{3+}$ cluster (calculated $m/z = 864.8264$), which is in good agreement with the theoretical isotopic distribution and provides

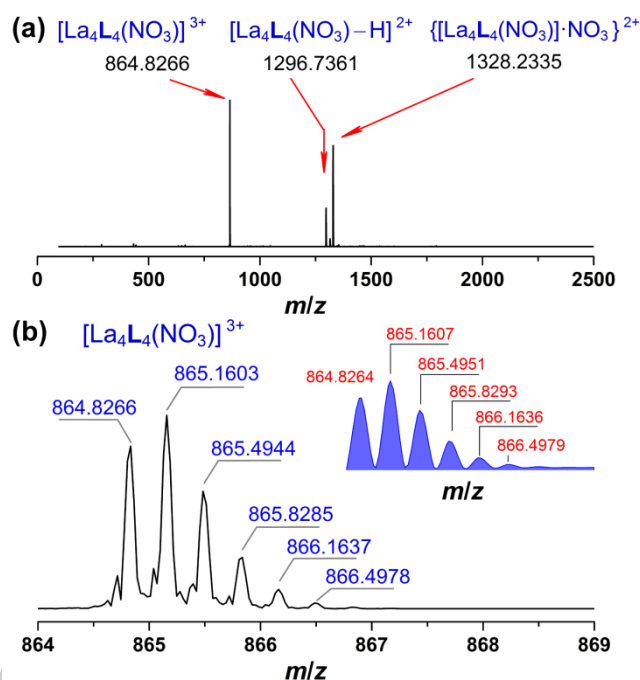


Figure 2. a) HRESI mass spectra of **1a** in methanol and the assignments of spectral peaks. b) Magnification of the mass peaks at $m/z = 864.8266$ with isotopic distribution patterns separated by $(0.33 \pm 0.005)\text{ Da}$. Inset: Theoretical HRESI mass spectra of $[\text{La}_4\{(R)\text{-L}\}_4(\text{NO}_3)]^{3+}$ at $m/z = 864.8264$ and isotopic distribution patterns.

directly evidence for the formation of stable chiral lanthanide quadruple-stranded helicates encapsulated with nitrate anion in the solution. Moreover, the mass peaks at $m/z = 1328.2335$ and 1296.7361 with isotopic distribution patterns separated by $(0.50 \pm 0.005)\text{ Da}$ can be attributed to the derivative ions of helicates $\{[\text{La}_4\{(R)\text{-L}\}_4(\text{NO}_3)]\cdot\text{NO}_3\}^{2+}$ (calculated $m/z = 1328.2336$) and $[\text{La}_4\{(R)\text{-L}\}_4(\text{NO}_3)\text{-H}]^{2+}$ (calculated $m/z = 1296.7358$), respectively (Figure S4 and Figure S5).

Chiral analysis of lanthanide helicates

To study the effects of chiral ligand on self-assembly of lanthanide helicates and understand the remarkable chirality transfer process from the ligand to cluster, the homochiral **1b** was prepared by employing (*S*)- H_2L in place of (*R*)- H_2L . As expected, the crystal of enantiomer $[\text{La}_4\{(S)\text{-L}\}_4(\text{NO}_3)]^{3+}$ was successfully obtained, and four ligands form a tetranuclear quadruple-stranded helix as well as **1a**, but with the opposite *F* helical configuration (Figure 3a, Figure S6). However, when racemic compound H_2L , with equal amounts of chiral (*R*)- H_2L and (*S*)- H_2L , was selected as ligand, we also could get tetranuclear quadruple-stranded lanthanide clusters under the same conditions, but they crystallized in achiral and centrosymmetric space group $P\bar{1}$. In complex **1**, two kinds of lanthanide helicates with *M* helical configuration and *P* helical configuration arranged and self-assembled alternatively in three

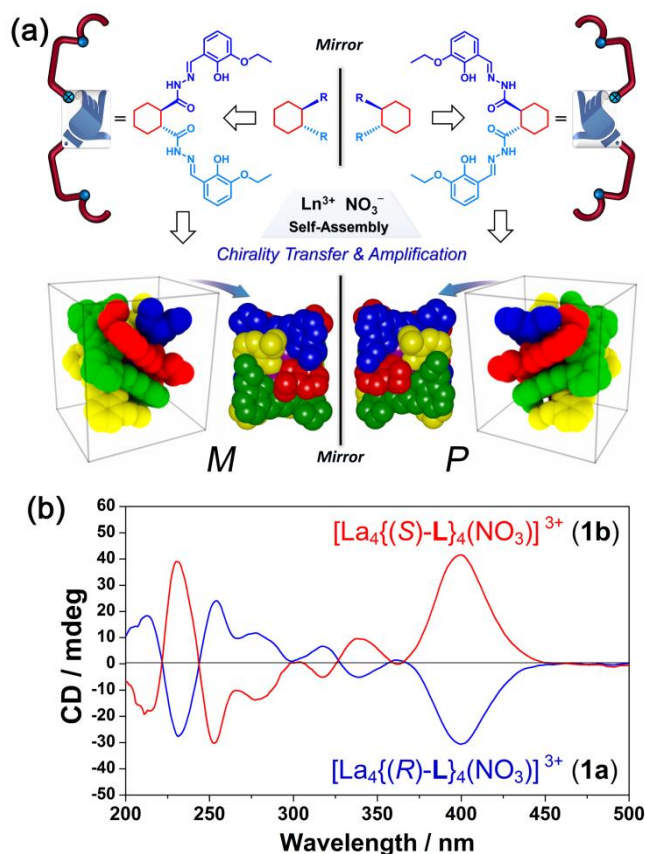


Figure 3. a) Molecular configurations and the relationship with the mirror image of two chiral bridging ligands (R)- H_2L (left) and (S)- H_2L (right), which could self-assemble respectively with lanthanide ions to form corresponding M and P helical tetranuclear quadruple-stranded clusters. Two helicates with mirror image are shown in a space-filling representation, and the chiral information of ligands is transferred and amplified. Hydrogen atoms, solvent molecules and uncoordinated anions are omitted for clarity. Each ligand is represented in a different color and the lanthanide ions are shown in violet. b) Solid-state CD spectra of **1a** and **1b** in KCl pellets, which present mirror image.

dimensions to form racemic supramolecule (Figure S7). As confirmed by solid-state circular dichroism (CD) spectroscopy, crystals of both **1a** and **1b** in KCl pellets exhibited stronger circular dichroism signals with positive and negative Cotton effect, respectively, which present mirror-image CD spectra with opposite signs (Figure 3b). But there is no any signal for **1** in CD spectra due to the ordered packing of two kinds of different helicates. Therefore, the chirality and purity of ligands could be preserved and transferred effectively towards complex helical system.

Recognition of chiral lanthanide helicates

The prominent structural stability and optical pure chiral features of these lanthanide tetranuclear quadruple-stranded helicates intrigued us to further explore their sensing applications based on chiral signal. Considering that there are a lot of hydrogen

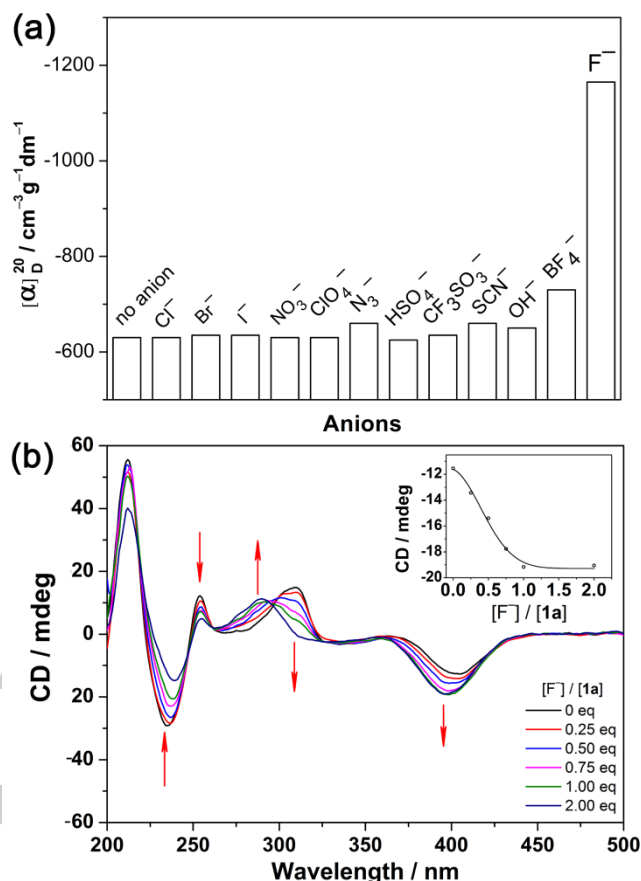


Figure 4. a) Optical rotation responses of **1a** to different anions in methanol. $\lambda = 589 \text{ nm}$, $[\text{1a}] = 4 \times [\text{anion}] = 4 \times 10^{-3} \text{ M}$. b) The CD change of **1a** upon addition F^- in methanol. Inset: The CD intensity at 400 nm as a function of $[\text{F}^-]/[\text{1a}]$. $[\text{1a}] = 5 \times 10^{-4} \text{ M}$.

bond donors in acylhydrazone groups and uncoordinated counter anions (Table S2), the responses of homochiral lanthanide helicates on different anions in optical rotation and circular dichroism (CD) spectra were subsequently investigated in solution. We measured the optical rotation of **1a** in methanol solution in the presence of F^- , Cl^- , Br^- , I^- , NO_3^- , BF_4^- , ClO_4^- , N_3^- , SCN^- , CF_3SO_3^- , OH^- and HSO_4^- , respectively. The results showed that a significant enhancement in optical rotation could be observed only for F^- , but no clear change for other anions in the same conditions, which suggested that F^- anion with strong electronegativity might take part in the exchange of counter anions and the formation of hydrogen bonds so that the optical rotation value of chiral **1a** was changed and magnified (Figure 4a). CD spectra of **1a** in methanol solution at the range of 200–500 nm also exhibited the selective response only for F^- . As shown as Figure 4b, the CD intensity of **1a** at 254, 308 and 400 nm decreased gradually but the CD intensity at 235 and 280 nm increased with the increase of F^- , which stopped changing further when two equiv F^- were added and accompanied by the formation of three isosbestic points at 247, 262 and 297 nm. These results clearly suggested that the introduction of F^- could

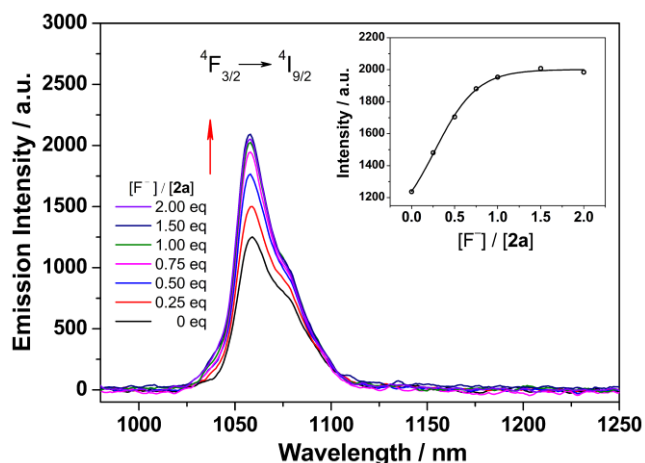


Figure 5. The NIR emission spectra change of **2a** upon addition F^- (0-2 equiv) in acetonitrile. Inset: The emission intensity of **2a** at 1060 nm as a function of $[F^-]/[2a]$. $[2a] = 1.0 \times 10^{-4}$ M, $\lambda_{ex} = 380$ nm.

influence the aggregation of chiral helicates and cause the change of chiral signal of helicates. Thus, optical rotation and CD analysis of the chiral lanthanide helicates, as simply and sensitively new tools, could be applied to F^- anion selective-recognition, which has not been reported to date.

On the other hand, as an important near-infrared (NIR) materials, Nd^{3+} ion with its sharp emission band centered at 1060 nm could be identified specifically and has potential applications in night vision, energy conversion, tracking, sensing, optical communication, anti-counterfeiting printing, and so on.^[16] Two enantiomeric homochiral tetranuclear quadruple-stranded helicates **2a** and **2b** were also self-assembled by Nd^{3+} ions and corresponding chiral ligands, respectively (Figure S8 and S9), and the chirality of ligand played a vital role for structural feature of homochiral helicate (Figure S10). **2a** exhibited strong characteristic emission of the Nd^{3+} ion at 1025-1125 nm, which can be assigned to the $^4F_{3/2} \rightarrow ^4I_{9/2}$ transition, pointing toward efficient sensitization of Nd^{3+} ion. The sensing property of **2a** towards F^- was monitored in methanol, and it exhibited chiral responses similar to **1a** in optical rotation and CD spectra (Figure S11 and S12). More importantly, the luminescent spectra of **2a** showed that the characteristic luminescent intensity of Nd^{3+} at 1060 nm increased rapidly with the amount of F^- until two equiv F^- were added (Figure 5), a turn-on near-infrared luminescent response toward F^- was observed clearly that is rarely reported now.

On the basis of the above results, a sensing model of the homochiral tetranuclear lanthanide helicates toward F^- anion might be proposed that involves the formation of hydrogen bonds and supramolecular self-assembly of helicates. In solution, F^- anions possess strong electronegativity and they could exchange with uncoordinated NO_3^- anions to approach acylhydrazone groups in ligand and form many strong $N-H \cdots F$ hydrogen bonds, which may lead to the aggregation or self-assembly of chiral helicates to some extent (Figure 6). The supramolecular interactions between helicates and F^- anions not only results in the change of chiral signals of helicates both in

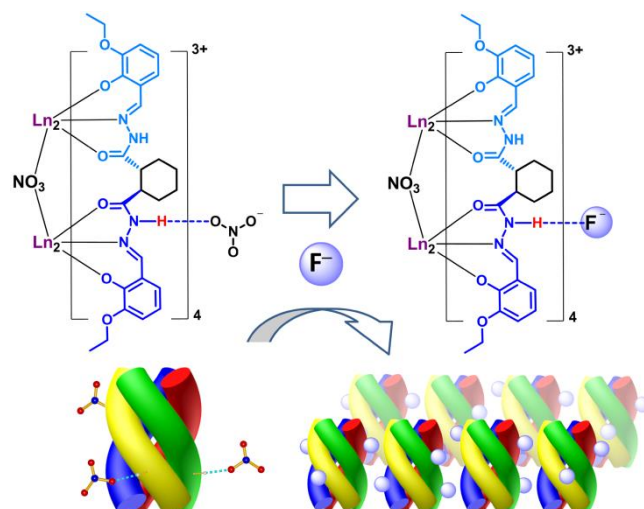


Figure 6. The recognition mechanism of chiral lanthanide-based tetranuclear helicates for F^- anion. The uncoordinated NO_3^- anions around the helicate could be replaced with F^- anions to form strong $N-H \cdots F$ hydrogen bonds and induce aggregation or supramolecular self-assembly of many chiral helicates. Hydrogen bonds are denoted by blue broken line.

optical rotation and CD spectra, but also could stabilize the structure of lanthanide helicates to weaken non-radiative transitions of Nd^{3+} ion, showing turn-on NIR luminescent response. Therefore, the lanthanide helicates displayed recognition of multi-model responses toward F^- anion both in chiral signal and NIR luminescence, which provides a meaningful exploitation of the lanthanide supramolecular structure and function.

Conclusions

In conclusion, we have designed a pair of chiral bridging ligands by the introduction of enantiomerically pure cyclohexyl group, which could effectively coordinate and self-assemble with lanthanide ions to form enantiomerically pure chiral lanthanide-based tetranuclear quadruple-stranded helicates with the aid of NO_3^- anion template under mild conditions. The self-assembly process of these unique chiral helicates not only ensured the structural stability and quadruple-stranded feature of lanthanide cluster in solid and solution, but also achieved the effective transfer and amplification of chirality code from ligand to higher supramolecular level. Meanwhile, through using optical rotation, CD spectra analysis and luminescence measurement, we found that the chiral lanthanide helicates could serve as sensitive and multi-responsive sensors to recognize and detect F^- based on the change of chiral signal and NIR luminescence simultaneously, which represents an innovative and meaningful exploration for the chiral lanthanide supramolecular structure and function. Thus, the understanding of self-assembly mechanism based on chiral transfer might be able to bring more opportunity to develop functional lanthanide-based polynuclear clusters.

Experimental Section

Materials and instrumentation: All the materials for synthesis were purchased from commercial suppliers and used without further purification. All of the solvents used were of analytical reagent grade and deionized water was used. ^1H NMR and ^{13}C NMR spectra were recorded on a JNM-ECS-400 MHz spectrometer and the chemical shift in ppm and using tetramethylsilane as internal reference. Mass spectra (ESI) for organic compounds were performed on a Bruker Daltonics Esquire 6000 mass spectrometer. HRESI-MS for complexes were performed on Fourier Transform Ion Cyclotron Resonance Mass Spectrometer. FT-IR spectra were recorded in KBr pellets on a NEXUS 670 in the region 4000–400 cm^{-1} . Elemental analyses (C, H, N) were performed on a Vario EL elemental analyzer. Solid-state ^{15}N high-power decoupling (HPDEC) NMR spectra were performed with a 4-mm double-resonance MAS probe on Bruker Avance II WB 400 MHz spectrometer. The solution CD spectra were recorded on an Olis DSM 1000 spectropolarimeter. Solid-state CD spectra measurements were performed on a JASCO J-810W spectrophotometer at room temperature. The steady-state luminescence spectra were performed on Edinburgh Instrument FSL920 fluorescence spectrometer. Optical rotations were measured at 20 °C in methanol on a Perkin-Elmer Model 341 polarimeter.

Synthesis of homochiral ligands

Synthesis of ligand (*R*)-H₂L: (1*R*,2*R*)-Cyclohexane-1,2-dicarbohydrazide was prepared first according to Scheme S1. To a solution of (1*R*,2*R*)-cyclohexane-1,2-dicarbohydrazide (0.80 g, 4.0 mmol) in ethanol (25 mL) was added 3-ethoxy-2-hydroxybenzaldehyde (1.36 g, 8.2 mmol) in ethanol (10 mL). This mixture was then stirred and allowed to stand for 6 h at 40 °C. The white precipitate was filtered off and washed with diethyl ether, and dried in vacuo to obtain ligand (*R*)-H₂L as white solid (1.60 g, yield 80.5 %). m.p. 247.6–248.5 °C. $[\alpha]_D^{20} = -29.0 \text{ cm}^3 \text{ g}^{-1} \text{ dm}^{-1}$ (The ligand exhibited poor solubility, which could be dissolved by addition of NaOH to become (*R*)-Na₂L, $c = 0.01 \text{ g cm}^{-3}$ (*R*)-Na₂L in methanol). ^1H NMR (400 MHz, DMSO-*d*₆): $\delta = 11.72$ (d, $J = 16.4$ Hz, 1.40H), 11.14 (s, 0.6H), 10.83 (d, $J = 21.6$ Hz, 1.4H), 9.54 (d, $J = 21.2$ Hz, 0.6H), 8.32 (d, $J = 22.0$ Hz, 2H), 6.78–7.20 (m, 6H), 4.02–4.08 (m, 4H), 2.50–2.63 (m, 1.4H), 1.79–2.05 (m, 4H), 1.30–1.38 (m, 10H). ^{13}C NMR (100 MHz, DMSO-*d*₆): $\delta = 175.57$, 171.01, 170.69, 147.44, 147.20, 147.10, 146.73, 146.50, 146.32, 141.65, 121.11, 120.39, 119.48, 119.08, 115.20, 114.17, 64.22, 44.11, 43.88, 41.58, 29.72, 28.49, 25.47, 25.20, 14.90, 14.83. ESI-MS m/z : calcd. for C₂₆H₃₂N₄O₆ 496.2322 and C₂₆H₃₂N₄O₆Na 519.2220, found: 519.2217 [M+Na]⁺. IR (KBr, cm^{-1}): 3435 (br), 3203 (m), 3060 (m), 2979 (m), 2929 (s), 2859 (m), 1655 (vs), 1609 (m), 1576 (w), 1547 (s), 1464 (vs), 1389 (s), 1353 (w), 1264 (w), 1248 (vs), 1190 (m), 1115 (m), 1077 (m), 1050 (w), 957 (w), 936 (w), 897 (w), 833 (w), 780 (w), 733 (s), 639 (w).

Synthesis of ligand (*S*)-H₂L: The enantiomer (*S*)-H₂L was prepared by the same procedure as that for (*R*)-H₂L, except that (1*S*,2*S*)-cyclohexane-1,2-dicarboxylic acid was used instead of the starting material (1*R*,2*R*)-cyclohexane-1,2-dicarboxylic acid. The enantiomer (*S*)-H₂L was obtained as white solid in 42.0 % total yield (3-Step reactions with (1*S*,2*S*)-cyclohexane-1,2-dicarboxylic acid as the starting material). $[\alpha]_D^{20} = +29.0 \text{ cm}^3 \text{ g}^{-1} \text{ dm}^{-1}$ (The ligand exhibited poor solubility, which could be dissolved by addition of NaOH to become (*S*)-Na₂L, $c = 0.01 \text{ g cm}^{-3}$ (*S*)-Na₂L in methanol). IR (KBr, cm^{-1}): 3434 (br), 3210 (m), 3060 (m), 2979 (m), 2929 (s), 2859 (m), 1656 (vs), 1609 (m), 1577 (w), 1546 (s), 1464 (vs), 1388 (s), 1353 (w), 1264 (w), 1248 (vs), 1190 (m), 1115 (m), 1077 (m), 1051 (w), 960 (w), 936 (w), 897 (w), 833 (w), 780 (w), 732 (s), 637 (w).

Synthesis of complexes

[La₄{(*R*)-L₄(NO₃)₃}]·3NO₃·*x*CH₃OH·*y*H₂O·*z*CH₃CN (1a**):** A mixture of LiOH·H₂O (4.2 mg, 0.1 mmol) and (*R*)-H₂L (24.8 mg, 0.05 mmol) in methanol (3 mL) was stirred for 5 min, then a solution of La(NO₃)₃·6H₂O (21.7 mg, 0.05 mmol) in methanol and acetonitrile (2 mL, *v/v*, 2:1) was added and the mixture was rapidly stirred for 5 min. The yellow crystals suitable for X-ray analysis were obtained 65 % yield by slow evaporation of the solution within one week at room temperature in air. Elemental analysis (%) calcd. for complex **1a** C₁₀₄H₁₂₀La₄N₂₀O₃₆ (non-coordinated solvent molecules were lost upon drying): C 44.90, H 4.35, N 10.07; found: C 44.79, H 4.25, N 10.15. HRESI-MS m/z : 864.8266 [La₄{(*R*)-L₄(NO₃)₃}]³⁺ (calcd. for C₁₀₄H₁₂₀La₄N₁₇O₂₇, 864.8264), 1296.7361 [La₄{(*R*)-L₄(NO₃)₃-H]²⁺ (calcd. for C₁₀₄H₁₁₉La₄N₁₇O₂₇, 1296.7358), 1328.2335 {[La₄{(*R*)-L₄(NO₃)₃}]·NO₃}²⁺ (calcd. for C₁₀₄H₁₂₀La₄N₁₈O₃₀, 1328.2336). IR (KBr, cm^{-1}): 3436 (br), 3226 (m), 3052 (w), 2975 (w), 2931 (m), 2860 (w), 1631 (m), 1605 (vs), 1556 (s), 1450 (s), 1384 (vs), 1304 (s), 1262 (w), 1219 (vs), 1174 (m), 1112 (w), 1096 (w), 1070 (m), 1044 (w), 938 (w), 891 (m), 855 (w), 740 (s), 641 (w).

[La₄{(*S*)-L₄(NO₃)₃}]·3NO₃·*x*CH₃OH·*y*H₂O·*z*CH₃CN (1b**):** The enantiomer **1b** was synthesized by the same procedure as that for **1a**, except that (*S*)-H₂L was used instead of (*R*)-H₂L. The crystals of **1b** were obtained in 62 % yield by slow evaporation of the mixed solution within one week at room temperature in air. Elemental analysis (%) calcd. for complex **1b** C₁₀₄H₁₂₀La₄N₂₀O₃₆ (non-coordinated solvent molecules were lost upon drying): C 44.90, H 4.35, N 10.07; found: C 44.74, H 4.30, N 9.95. IR (KBr, cm^{-1}): 3436 (br), 3240 (m), 3053 (w), 2975 (w), 2931 (m), 2860 (w), 1632 (m), 1605 (vs), 1555 (s), 1450 (s), 1384 (vs), 1307 (s), 1261 (w), 1219 (vs), 1174 (m), 1113 (w), 1095 (w), 1070 (m), 1044 (w), 938 (w), 891 (m), 855 (w), 741 (s), 642 (w).

[La₄L₄(NO₃)₃]·3NO₃·*x*CH₃OH·*y*H₂O·*z*CH₃CN (1**):** The racemic **1** was synthesized by the same procedure as that for **1a**, except that the racemic mixture of (*R*)-H₂L and (*S*)-H₂L was used instead of chiral (*R*)-H₂L. The crystals of **1** were obtained in 58 % yield by slow evaporation of the mixed solution within one week at room temperature in air. Elemental analysis (%) calcd. for complex **1** C₁₀₄H₁₂₀La₄N₂₀O₃₆ (non-coordinated solvent molecules were lost upon drying): C 44.90, H 4.35, N 10.07; found: C 44.80, H 4.23, N 10.16. IR (KBr, cm^{-1}): 3436 (br), 3240 (m), 3053 (w), 2975 (w), 2931 (m), 2860 (w), 1632 (m), 1605 (vs), 1555 (s), 1450 (s), 1384 (vs), 1307 (s), 1261 (w), 1219 (vs), 1174 (m), 1113 (w), 1095 (w), 1070 (m), 1044 (w), 938 (w), 891 (m), 855 (w), 741 (s), 642 (w).

[Nd₄{(*R*)-L₄(NO₃)₃}]·3NO₃·*x*CH₃OH·*y*H₂O·*z*CH₃CN (2a**):** Complex **2a** was synthesized by the same procedure as that for **1a**, except that Nd(NO₃)₃·6H₂O was used instead of La(NO₃)₃·6H₂O. The crystals of **2a** were obtained in 58 % yield by slow evaporation of the mixed solution within one week at room temperature in air. Elemental analysis (%) calcd. for complex **2a** C₁₀₄H₁₂₀Nd₄N₂₀O₃₆ (non-coordinated solvent molecules were lost upon drying): C 44.56, H 4.31, N 9.99; found: C 44.78, H 4.20, N 9.98. IR (KBr, cm^{-1}): 3437 (br), 3205 (m), 3051 (w), 2975 (w), 2930 (m), 2859 (w), 1631 (m), 1605 (vs), 1557 (s), 1448 (s), 1384 (vs), 1301 (s), 1263 (w), 1221 (vs), 1174 (m), 1097 (w), 1070 (m), 1043 (w), 938 (w), 892 (m), 856 (w), 741 (s), 642 (w).

[Nd₄{(*S*)-L₄(NO₃)₃}]·3NO₃·*x*CH₃OH·*y*H₂O·*z*CH₃CN (2b**):** The enantiomer **2b** was synthesized by the same procedure as that for **2a**, except that (*S*)-H₂L was used instead of (*R*)-H₂L. The crystals of **2b** were obtained in 53 % yield by slow evaporation of the mixed solution within one week at room temperature in air. Elemental analysis (%) calcd. for complex **2b** C₁₀₄H₁₂₀Nd₄N₂₀O₃₆ (non-coordinated solvent molecules were lost upon drying): C 44.56, H 4.31, N 9.99; found: C 44.85, H 4.52, N 10.15. IR (KBr, cm^{-1}): 3437 (br), 3212 (m), 3052 (w), 2975 (w), 2930 (m), 2859 (w),

1631 (m), 1605 (vs), 1557 (s), 1448 (s), 1384 (vs), 1302 (s), 1263 (w), 1220 (vs), 1174 (m), 1097 (w), 1070 (m), 1043 (w), 938 (w), 891 (m), 855 (w), 741 (s), 642 (w).

Single crystal X-ray crystallography: Single-crystal X-ray diffraction measurements were carried out on a Bruker SMART APEX-II CCD diffractometer (**1a**, **1b**, **1**) and an Agilent SuperNova system (**2a**, **2b**) using a microfocus sealed-tube X-ray source with graphite monochromated Mo K α ($\lambda = 0.71073$ Å) radiation. Multi-scan absorption correction was applied with the SADABS program. Unit cell dimensions were obtained with least-squares refinements, and all structures were solved by direct methods using SHELXS-97.^[17] Metal atoms in each complex were located from *E*-maps. The non-hydrogen atoms were located in successive difference Fourier syntheses. The final refinement was performed by full matrix least-squares methods with anisotropic thermal parameters for non-hydrogen atoms on F^2 . The hydrogen atoms were introduced at calculated positions and not refined (riding model). In all structures, disordered groups or molecules were split reasonably, and no attempt was made to locate the hydrogen atoms of the disordered water molecules. Crystallographic data as well as details of data collection and refinement for all complexes are summarized in Table S1, whereas selected bond lengths and angles are listed in Table S2. CCDC 1523289-1523293 contain the supplementary crystallographic data for this paper. These data can be obtained free of charge from The Cambridge Crystallographic Data Centre via www.ccdc.cam.ac.uk/data_request/cif.

Acknowledgements

This work was supported by NSFC (Grant 21371083, 21431002) and the Fundamental Research Funds for the Central Universities (lzujbky-2015-k04).

Keywords: self-assembly • helicates • lanthanides • chiral recognition • fluoride

- [1] a) M. Gardner, *The New Ambidextrous Universe*, 3rd ed., W. H. Freeman, New York, 1990; b) W. J. Lough, I. W. Wainer, *Chirality in Natural and Applied Science*, Blackwell Scientific, Oxford, 2002; c) R. Kuroda, B. Endo, M. Abe, M. Shimizu, *Nature* **2009**, *462*, 790-794.
- [2] a) J. J. L. M. Cornelissen, A. E. Rowan, R. J. M. Nolte, N. A. J. M. Sommerdijk, *Chem. Rev.* **2001**, *101*, 4039-4070; b) J. L. Sun, C. Bonneau, A. Cantin, A. Corma, M. J. Diaz-Cabanas, M. Moliner, D. L. Zhang, M. R. Li, X. D. Zou, *Nature* **2009**, *458*, 1154-1157; c) M. Liu, L. Zhang, T. Wang, *Chem. Rev.* **2015**, *115*, 7304-7397; d) Z. Gu, C. Zhan, J. Zhang, X. Bu, *Chem. Soc. Rev.* **2016**, *45*, 3122-3144.
- [3] a) J. S. Seo, D. Whang, H. Lee, S. I. Jun, J. Oh, Y. J. Jeon, K. Kim, *Nature* **2000**, *404*, 982-986; b) V. Farina, J. T. Reeves, C. H. Senanayake, J. J. Song, *Chem. Rev.* **2006**, *106*, 2734-2793; c) Y. Okamoto, T. Ikai, *Chem. Soc. Rev.* **2008**, *37*, 2593-2608; d) I. Aillaud, J. Collin, C. Duhayon, R. Guillot, D. Lyubov, E. Schulz, A. Trifonov, *Chem. Eur. J.* **2008**, *14*, 2189-2200; e) G. Li, W. Yu, J. Ni, T. Liu, Y. Liu, E. Sheng, Y. Cui, *Angew. Chem. Int. Ed.* **2008**, *47*, 1245-1249; *Angew. Chem.* **2008**, *120*, 1265-1269; f) M. Yoon, R. Srirambalaji, K. Kim, *Chem. Rev.* **2012**, *112*, 1196-1231; g) G. Liu, D. Zhang, C. Feng, *Angew. Chem. Int. Ed.* **2014**, *53*, 7789-7793; *Angew. Chem.* **2014**, *126*, 7923-7927; h) J. Shen, Y. Okamoto, *Chem. Rev.* **2016**, *116*, 1094-1138; i) P. G. Lacroix, I. Malfant, C. Lepetit, *Coord. Chem. Rev.* **2016**, *308*, 381-394.
- [4] a) B. Kesanli, W. Lin, *Coord. Chem. Rev.* **2003**, *246*, 305-326; b) J. Crassous, *Chem. Soc. Rev.* **2009**, *38*, 830-845; c) L. Ma, C. Abney, W. Lin, *Chem. Soc. Rev.* **2009**, *38*, 1248-1256; d) E. B. Bauer, *Chem. Soc. Rev.* **2012**, *41*, 3153-3167; e) A. M. Castilla, W. J. Ramsay, J. R. Nitschke, *Acc. Chem. Res.* **2014**, *47*, 2063-2073; f) S. Y. Zhang, D. Li, D. Guo, H. Zhang, W. Shi, P. Cheng, L. Wojtas, M. J. Zaworotko, *J. Am. Chem. Soc.* **2015**, *137*, 15406-15409; g) A. Aliprandi, C. M. Croisetu, M. Mauro, L. D. Cola, *Chem. Eur. J.* **2017**, *23*, 1-6.
- [5] a) C. Piguat, G. Bernardinelli, G. Hopfgartner, *Chem. Rev.* **1997**, *97*, 2005-2062; b) M. Albrecht, *Chem. Rev.* **2001**, *101*, 3457-3498; c) M. Albrecht, *Angew. Chem. Int. Ed.* **2005**, *44*, 6448-6451; *Angew. Chem.* **2005**, *117*, 6606-6609; d) M. Horie, N. Ousaka, D. Taura, E. Yashima, *Chem. Sci.* **2015**, *6*, 714-723; e) O. Gidron, M. Jirásek, M. Wörle, F. Diederich, *Chem. Eur. J.* **2016**, *22*, 16172-16177.
- [6] a) A. V. Davis, D. Fiedler, M. Ziegler, A. Terpin, K. N. Raymond, *J. Am. Chem. Soc.* **2007**, *129*, 15354-15363; b) R. Chakrabarty, P. S. Mukherjee, P. J. Stang, *Chem. Rev.* **2011**, *111*, 6810-6918; c) H. Amouri, C. Desmarests, J. Moussa, *Chem. Rev.* **2012**, *112*, 2015-2041; d) C. J. Brown, F. D. Toste, R. G. Bergman, K. N. Raymond, *Chem. Rev.* **2015**, *115*, 3012-3035; e) W. M. Bloch, Y. Abe, J. J. Holstein, C. M. Wandtke, B. Dittrich, G. H. Clever, *J. Am. Chem. Soc.* **2016**, *138*, 13750-13755.
- [7] a) W. L. Leong, J. J. Vittal, *Chem. Rev.* **2011**, *111*, 688-764; b) C. He, D. Liu, W. Lin, *Chem. Rev.* **2015**, *115*, 11079-11108.
- [8] a) C. D. Wu, A. Hu, L. Zhang, W. Lin, *J. Am. Chem. Soc.* **2005**, *127*, 8940-8941; b) H. Y. Li, L. Jiang, H. Xiang, T. A. Makal, H. C. Zhou, T. B. Lu, *Inorg. Chem.* **2011**, *50*, 3177-3179; c) W. Lu, Z. Wei, Z. Gu, T. Liu, J. Park, J. Park, J. Tian, M. Zhang, Q. Zhang, T. Gentle III, M. Bosch, H. Zhou, *Chem. Soc. Rev.* **2014**, *43*, 5561-5593; d) S. Lee, E. A. Kapustin, O. M. Yaghi, *Science* **2016**, *353*, 808-811.
- [9] a) K. S. Jeong, Y. S. Kim, Y. J. Kim, E. Lee, J. H. Yoon, W. H. Park, Y. W. Park, S.-J. Jeon, Z. H. Kim, J. Kim, N. Jeong, *Angew. Chem. Int. Ed.* **2006**, *45*, 8134-8138; *Angew. Chem.* **2006**, *118*, 8314-8318; b) X. L. Tang, W. H. Wang, W. Dou, J. Jiang, W. S. Liu, W. W. Qin, G. L. Zhang, H. R. Zhang, K. B. Yu, L. M. Zheng, *Angew. Chem. Int. Ed.* **2009**, *48*, 3499-3502; *Angew. Chem.* **2009**, *121*, 3551-3554; c) X. J. Kong, L. S. Long, Z. Zheng, R. B. Huang, L. S. Zheng, *Acc. Chem. Res.* **2010**, *43*, 201-209; d) G. Bozoklu, C. Gateau, D. Imbert, J. Pécaut, K. Robeyns, Y. Filinchuk, F. Memon, G. Muller, M. Mazzanti, *J. Am. Chem. Soc.* **2012**, *134*, 8372-8375; e) W. Liu, X. Tang, *Struct. Bonding*, **2014**, *163*, 29-74; f) D. E. Barry, D. F. Caffrey, T. Gunnlaugsson, *Chem. Soc. Rev.* **2016**, *45*, 3244-3274; g) A. Galanti, O. Kotova, S. Blasco, C. J. Johnson, R. D. Peacock, S. Mills, J. J. Boland, M. Albrecht, T. Gunnlaugsson, *Chem. Eur. J.* **2016**, *22*, 9709-9723.
- [10] a) J. C. G. Bünzli, C. Piguat, *Chem. Soc. Rev.* **2005**, *34*, 1048-1077; b) S. V. Eliseeva, J. C. G. Bünzli, *Chem. Soc. Rev.* **2010**, *39*, 189-227; c) D. N. Woodruff, R. E. Winpenny, R. A. Layfield, *Chem. Rev.* **2013**, *113*, 5110-5148; d) O. Kotova, S. Blasco, B. Twamley, J. O'Brien, R. D. Peacock, J. A. Kitchen, M. Martinez-Calvo, T. Gunnlaugsson, *Chem. Sci.* **2015**, *6*, 457-471.
- [11] See, for example: a) C. Piguat, A. F. Williams, G. Bernardinelli, *Angew. Chem. Int. Ed.* **1992**, *31*, 1622-1624; *Angew. Chem.* **1992**, *104*, 1626-1628; b) J.-M. Lehn, *Science* **2002**, *295*, 2400-2403; c) J. Hamacek, S. Blanc, M. Elhabiri, E. Leize, A. Van Dorsselaer, C. Piguat, A. M. Albrecht-Gary, *J. Am. Chem. Soc.* **2003**, *125*, 1541-1550; d) K. Zeckert, J. Hamacek, J. M. Senegas, N. Dalla-Favera, S. Floquet, G. Bernardinelli, C. Piguat, *Angew. Chem. Int. Ed.* **2005**, *44*, 7954-7958; *Angew. Chem.* **2005**, *117*, 8168-8172; e) T. B. Jensen, R. Scopelliti, J. C. G. Bünzli, *Inorg. Chem.* **2006**, *45*, 7806-7814; f) M. Albrecht, O. Osetska, J. C. G. Bünzli, F. Gumy, R. Fröhlich, *Chem. Eur. J.* **2009**, *15*, 8791-8799; g) B. E. Aroussi, S. Zebret, C. Besnard, P. Perrottet, J. Hamacek, *J. Am. Chem. Soc.* **2011**, *133*, 10764-10767.
- [12] a) T. Gunnlaugsson, M. Glynn, G. M. Tocci, P. E. Kruger, F. M. Pfeffer, *Coord. Chem. Rev.* **2006**, *250*, 3094-3117; b) E. L. Que, D. W. Domaille, C. J. Chang, *Chem. Rev.* **2008**, *108*, 1517-1549; c) P. Ballester, *Chem. Soc. Rev.* **2010**, *39*, 3810-3830; d) Y. Yang, Q. Zhao,

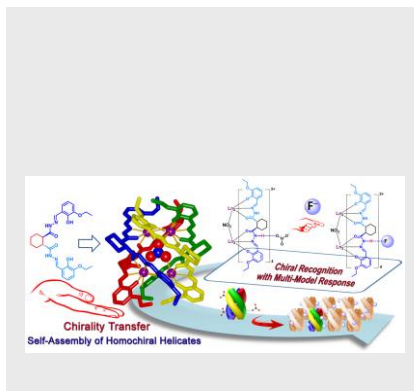
- W. Feng, F. Li, *Chem. Rev.* **2013**, *113*, 192-270; e) S. Lee, K. K. Yuen, K. A. Jolliffe, J. Yoon, *Chem. Soc. Rev.* **2015**, *44*, 1749-1762.
- [13] a) R. Sandhu, H. Lal, Z. S. Kundu, S. Kharb, *Bio. Trace Elem. Res.* **2011**, *144*, 1-5; b) M. Cametti, K. Rissanen, *Chem. Soc. Rev.* **2013**, *42*, 2016-2038.
- [14] a) V. Amendola, D. Esteban-Gomez, L. Fabbrizzi, M. Licchelli, *Acc. Chem. Res.* **2006**, *39*, 343-353; b) C. R. Wade, A. E. J. Broomsgrove, S. Aldridge, F. P. Gabbaï, *Chem. Rev.* **2010**, *110*, 3958-3984; c) Y. Zhou, J. F. Zhang, J. Yoon, *Chem. Rev.* **2014**, *114*, 5511-5571; d) N. Busschaert, C. Caltagirone, W. Van Rossom, P. A. Gale, *Chem. Rev.* **2015**, *115*, 8038-8155.
- [15] a) M. H. Lee, J. H. Han, P. S. Kwon, S. Bhuniya, J. Y. Kim, J. L. Sessler, C. Kang, J. S. Kim, *J. Am. Chem. Soc.* **2012**, *134*, 1316-1322; b) L. E. Santos-Figueroa, M. E. Moragues, E. Climent, A. Agostini, R. Martínez-Máñez, F. Sancenón, *Chem. Soc. Rev.* **2013**, *42*, 3489-3613; c) L. Gai, J. Mack, H. Lu, T. Nyokong, Z. Li, N. Kobayashi, Z. Shen, *Coord. Chem. Rev.* **2015**, *285*, 24-51.
- [16] a) J. C. G. Bünzli, *Chem. Rev.* **2010**, *110*, 2729-2755; b) F. Chen, Z. Chen, Z. Bian, C. Huang, *Coord. Chem. Rev.* **2010**, *254*, 991-1010; c) J. C. G. Bünzli, *Coord. Chem. Rev.* **2015**, *293-294*, 19-47.
- [17] G. M. Sheldrick, *Acta Crystallogr. Sect. A* **2008**, *64*, 112-122.

Entry for the Table of Contents

FULL PAPER

Homochiral Lanthanide Helicates:

Homochiral Lanthanide tetranuclear quadruple-stranded helicates were synthesized by chiral bridging ligands, which exhibit stable structure and achieve the effective transfer and amplification of chirality code. Meanwhile, the chiral lanthanide helicate could apply to F⁻ anions detection with multi-model responses both in chiral signal and NIR luminescence.



Wanmin Chen, Xiaoliang Tang,* Wei Dou, Bei Wang, Lirong Guo, Zhenghua Ju, and Weisheng Liu*

Page No. – Page No.

The Construction of Homochiral Lanthanide Quadruple-Stranded Helicates with Multi-Responsive Sensing Properties toward Fluoride Anions